THE JOURNAL OF PHYSICAL CHEMISTRY A

Article

pubs.acs.org/JPCA

Theoretical and Spectroscopic Analysis of *N,N′*-Diphenylurea and *N,N′*-Dimethyl-*N,N′*-diphenylurea Conformations

Jhenny F. Galan,*[,†] Edward Germany,[†] Amanda Pawlowski,[‡] Lynette Strickland,[†] and Mary Grace I. Galinato[‡]

[†]Department of Marine Sciences, Texas A&M University at Galveston, 200 Seawolf Parkway, Galveston, Texas 77553, United States

[‡]School of Science, Penn State Erie, The Behrend College, Erie, Pennsylvania 16563, United States

Supporting Information

ABSTRACT: Structural organization of macromolecules is highly dependent on the conformational propensity of the monomer units. Our goal is to systematically quantify differences in the conformational propensities of aromatic oligourea foldamer units. Specifically, we investigate the conformational propensities of *N,N′*-diphenylurea and *N,N′*-dimethyl-*N,N′*-diphenylurea in different media using a combination of theoretical methods, and infrared and nuclear magnetic resonance spectroscopies. Our results show variation in the conformational behavior upon adding methyl substituents on *N,N′*-diphenylurea, and varying the environments surrounding the compounds. Our energetic analyses and conformational distributions in the gas phase show predominance of the *cis*−*trans* and *trans*−*trans* conformations for *N,N′*-diphenylurea, while *cis*−*cis* conformation is favored for *N,N′*-dimethyl-*N,N′*-diphenylurea. In solution, our results support the *trans*−*trans* conformer as the predominant conformer for *N,N′*-diphenylurea, whereas the *cis*−*cis* and *cis*−*trans* forms are favored in *N,N′*-dimethyl-*N,N′*-diphenylurea. *N,N′*-Dimethyl-*N,N′*-diphenylurea also exhibits a more dynamic conformational behavior in solution, with constant fluctuations between *cis*−*cis* and *cis*−*trans* conformations. Our detailed quantitative analyses are an important aspect in fine-tuning desired conformations and dynamic properties of this class of oligomers by providing a molecular basis for the behavior at the monomeric level.

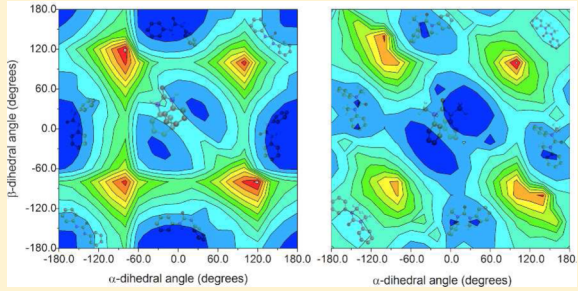

1. INTRODUCTION

The function and mechanism of action of naturally occurring biopolymers are highly dependent on their structural properties and arrangement. These attributes inspired the design and synthesis of foldamers, compounds known to adopt stable secondary structures in solution. Various foldamer types have been reported to fold into well-defined conformations such as helical, *β*-sheets, and macrocycles, mimicking bioactive molecules such as proteins and DNA.[1−4] Aromatic oligourea foldamers represent one class of foldamers whose basic motif consists of repeating units of phenyl and urea groups. Helical,[5−8] macrocyclic[8,9]and aromatic urea oligomers with switchable conformations[10] have been synthesized previously. Aromatic oligoureas are forced into a folded conformation by using directional interactions. For example, as shown in Figure 1, folding of aromatic oligourea foldamers are induced by intramolecular hydrogen bonding interaction (Figure 1B and 1C)[8] or addition of *N,N′*-substituents on the urea group. *N,N′*-substituted aromatic multilayered oligoureas (Figure 1A) with varying chain lengths are shown to exhibit helical properties by vibrational circular dichroism (CD) spectroscopy.[11,12] This group of helical oligourea foldamers has garnered attention due to the possibility of controlling helical handedness, in addition to stable helical structures with rigid backbones that mimic biological structures. Control of helicity in synthetic compounds offers vast possibilities in applications such as chemical sensing, and enantioselective catalysis.[13] Despite the rapidly growing advances in the design and synthesis of this class of compounds, the conformational behavior and dynamics of the folded oligomers remains unclear. Further, unlike biopolymers such as proteins, the lack of knowledge on the conformational behavior of oligomers is compounded two ways: (1) a deficiency in the systematic analyses of the structural features that govern certain conformations and (2) an insufficiency of molecular tools required to explore such analysis.

The conformation a foldamer adopts is partly driven by the inherent conformational propensity of the building blocks. In this study, we investigate the structural features and conformational behavior of building blocks of *N,N′*-substituted oligoureas, specifically *N,N′*-diphenylurea (**1**) and *N,N′*-dimethyl-*N,N′*-diphenylurea (**2**) (Figure 2, compounds **1** and **2**, respectively), using quantum mechanical (QM) methods, molecular dynamics (MD) simulations, and infrared (IR) and nuclear magnetic resonance (NMR) spectroscopies. Despite previous theoretical and experimental studies of the two compounds,[12,14−19] detailed quantitative study that provides

Received: April 10, 2014
Revised: June 26, 2014
Published: June 27, 2014

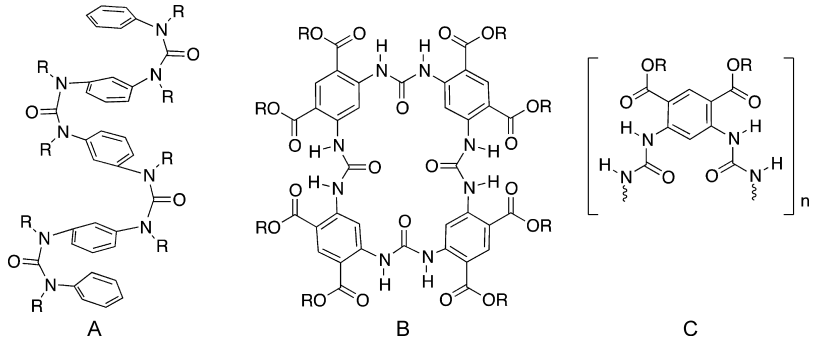

Figure 1. Structures of aromatic oligourea foldamers: (A) aromatic multilayered oligourea foldamer shown to exhibit helical properties.[6] The helical structure is induced by adding *N,N′*-substituents, forcing the folded *cis*−*cis* conformation of the urea group. Cyclic (B) and helical or crescent (C) aromatic oligourea foldamers stabilized by intramolecular H-bonding interaction between the *o*- and *p*-ester substituents of the urea group.[8]

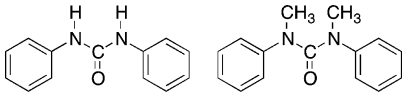

Figure 2. Structures of *N,N′*-diphenylurea (**1**) and *N,N′*-dimethyl-*N,N′*-diphenylurea (**2**).

molecular insights into the conformational propensities and solution dynamics of these compounds is still deficient. In particular, we present a detailed energetic analysis of compounds **1** and **2** using various theoretical methods and basis sets. The purpose of this part of the study is to find a robust and computationally efficient density functional method that accurately predicts properties of this class of compounds. This will serve as a basis for future theoretical and experimental work on more complex aromatic urea structures. We calculated the energies of the equilibrium conformations of the compounds as well as the two-dimensional (2-D) torsional energy profiles for rotation around the C−N bonds of the urea group using QM methods. MD simulations in conjunction with IR and NMR spectroscopies were carried out to quantify the conformational behavior of the compounds in different environments. Importantly, results on the propensities of the compounds provide physical insight into the stabilities of the conformers in the gas phase, solid state, and solution (e.g., chloroform and dimethyl sulfoxide (DMSO) solvents), as well as the dynamic behavior of compounds **1** and **2** as the molecular nature of the environment is varied.

2. MATERIALS AND METHODS

2.1. Computational Studies. *2.1.1. Quantum Mechanical Calculations.* We carried out a systematic basis set study on the calculated geometries and energies of compounds **1** and **2** to ensure computational efficiency and accuracy when employing quantum mechanical calculations on this group of compounds. We have carried out calculations at the HF, B3LYP, MP2, and B97D levels of theory, with triple-ζ basis sets and in some cases with diffuse functions. Supporting Information Tables S1 and S2 show representative geometrical parameters of *trans*−*trans N,N′*-diphenylurea and *cis*−*cis N,N′*-dimethyl-*N,N′*-diphenylurea, which are both stable conformers of the compounds, calculated using different QM methods. In general, for both compounds, the geometries obtained using the less expensive density functional theory (DFT) methods such as B3LYP and B97D are comparable to geometries obtained using MP2 at the highest basis set, 6-311G(2d,p). Previous convergence studies involving monomers of aromatic oligoamide foldamers have shown very similar results.[20,21] A detailed discussion is presented in Supporting Information (SI) section 1.

The relative energies of the preferred conformations of compounds **1** and **2** were obtained at the B3LYP,[22,23] MP2,[24−26] and B97D levels of theory with basis sets ranging from 6-311G(d,p) to 6-311++G** (Tables 1 and 2). Counterpoise corrections[27,28] to account for basis set superposition errors (BSSE) were calculated for geometries and energies at the MP2 level. The 2-D torsional energy profiles were calculated by scanning the torsional potential energy surface for rotation around each C_{urea}−N_{urea} bond in 20° increments using B97D/6-311G(d,p). At each scan point, all of the internal coordinates were optimized except for the dihedral angle defining the specific scan point.

Vibrational frequencies of the different conformations were determined at the B3LYP/6-311G(d,p) level of theory and used to aid in assignment of the experimental vibrational frequencies and normal modes. For the vibrational calculations, we opted for B3LYP/6-311G(d,p) since this method has been studied extensively for a wide range of compounds and has established frequency scaling factors that correlate well with experimental spectra. The scaling factor used in the reported vibrational frequencies is 0.968, which is based on the extensive study by Andersson and Uvdal[29] who employed 950 vibrational frequencies (belonging to 125 molecules) in their database. To our knowledge, no similar extensive studies were investigated to probe the accuracy of the B97D functional in predicting vibrational frequencies; therefore, we utilize B3LYP in the vibrational analysis.

All quantum mechanical calculations were performed using the Gaussian09 program.[30] Detailed NBO analyses of the various conformations were carried out using the NBO 6.0 program.[31,32]

2.1.2. Conformational Analysis. Conformational propensities of compounds **1** and **2** in different environments were calculated using the Boltzmann equation[33] and molecular dynamics simulations. We carried out 50 ns NVT MD simulations in gas phase, chloroform, and DMSO at 300 K. For solvent simulations, the equilibrated solvent box dimensions used were approximately 35 × 35 × 35 Å^3. The general Amber force field (GAFF)[34] and AMBER force field solvent parameters[35] were used in the simulations. Torsional parameters for rotation around the C_{urea}−N_{urea} bond were modified based on the QM torsional profiles obtained in this work (V = 6.6 kcal/mol for compound **1** and V = 7.2 kcal/mol

dx.doi.org/10.1021/jp503539m | J. Phys. Chem. A 2014, 118, 5304−5315

for compound **2**). We also modified the torsional parameter for rotation around the $C_{aromatic}-N_{urea}$ bond, known to be overestimated in the original GAFF parameter set.[21] All torsional parameter optimizations were based on previously published methodologies.[20,36,37] Partial charges were calculated using the RESP[38] charge fitting methodology using the equilibrium geometries of the compounds. All MD simulations were carried out using NAMD[39] (Theoretical and Computational Biophysics Group in the Beckman Institute for Advanced Science and Technology, University of Illinois at Urbana–Champaign).

2.2. IR Spectroscopy. Samples of *N,N′*-diphenylurea (Sigma-Aldrich, 98%) and *N,N′*-dimethyl-*N,N′*-diphenylurea (Santa Cruz Biotechnology, Inc., >98%) were obtained and used in the experiments. The mid-infrared spectra of the samples were collected on a Nicolet 6700 FT-IR spectrometer (Thermo Scientific) employing a KBr matrix for the solid samples and *trans*mission technique (CaF_2 windows) for the solutions. The spectral resolution was set at 4 cm^{-1}, and a total of 32 interferograms were averaged in each data collection. All measurements were performed at room temperature.

Lorentzian deconvolutions were performed on the IR spectra of both diphenylurea samples using the program PeakFit (version 4.0.6.0). The spectra were fit to the least number of Lorentzian functions, and the quality of the individual fits was monitored using χ^2. Bandwidths of the Lorentzian curves for each band were allowed to fluctuate no greater than 60 cm^{-1}. For each diphenylurea sample, the solid IR spectrum was best fit based on the presence of two possible conformations (see discussion that follows). The main peaks were fit and assigned to the most stable and experimentally verified conformations (*trans–trans* and *cis–cis* for **1** and **2**, respectively), while shoulders and weaker features were attributed to the less stable conformations (*cis–trans* for both **1** and **2**). Reiterations on the fitting procedure were performed until the sum of the fits was comparable to the experimentally determined spectrum. Population analyses on the solid IR spectra were accomplished by taking the ratios of the intensities of the conformers in the N–H stretching (for compound **1**) and C═O stretching (for compound **2**) regions, and then multiplying them against an internal standard (the calculated intensities).[40]

Normal mode assignment of the bands in the 500–3500 cm^{-1} region of the experimental IR spectra was achieved by correlating the vibrational frequencies to the theoretical data based on energy difference, intensity, and a previous study.[15]

2.3. NMR Spectroscopy. ^1H NMR spectra were recorded using a Bruker AVANCE 400 NMR spectrometer equipped with a BBO tunable multinuclear *z*-gradient probe. Solutions of *N,N′*-diphenylurea (13 mg/mL 90/10 v/v $CDCl_3$/DMSO-d_6; 26 mg/mL DMSO-d_6) and *N,N′*-dimethyl-*N,N′*-diphenylurea (24 mg/mL $CDCl_3$; 3 mg/mL DMSO-d_6) were prepared using tetramethylsilane as internal standard. Acquisition and processing of data were performed using TopSpin v.2.1 software package (Bruker Biosciences Corp.).

3. RESULTS AND DISCUSSION

The results and discussion presented as follows focus on the characterization of the conformational behavior of compounds **1** and **2** in terms of energetics and conformational distributions in different environments. The *trans* and *cis* structural nomenclature referred to in the following sections is based on the relative orientation of the amide group(s) in each conformer as shown in Figure 3. The equilibrium geometries of **1** and **2** at different levels of theory and basis sets have been systematically studied and are presented in detail in SI section 1.

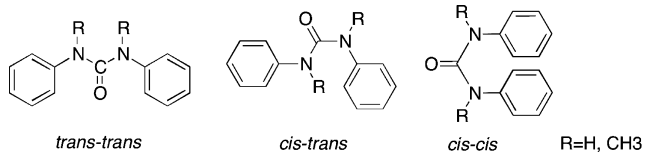

Figure 3. Conformers of *N,N′*-diphenylurea and *N,N′*-dimethyl-*N,N′*-diphenylurea.

3.1. Energetics of Conformations. Tables 1 and 2 show the relative energies in vacuum of the *trans–trans*, *cis–trans*, and *cis–cis* conformations (Figure 3) of compounds **1** and **2**, respectively, at different levels of theory. The equilibrium geometries were ensured to be at a minimum by performing frequency calculations.

With the exception of the MP2 level of theory (see discussion that follows), all levels of theory predict that *cis–trans* and *trans–trans* are the low-energy conformations of compound **1**, with *cis–trans* as the most stable structure while *cis–cis* is the least stable (Table 1). For geometries optimized at the MP2/6-311G(2d,p) level, recalculated energies using B3LYP show the *trans–trans* to be more stable. However, the energy differences between the two conformers are very small in all cases, which is ∼0.50 kcal/mol at the B3LYP level with different basis sets. It is worth noting that, at the MP2 level, the *trans–trans* structures have calculated relative energies of ∼2.0–2.5 kcal/mol higher than the *cis–trans* structure, while the *cis–cis* structures tend to be overstabilized. For the geometries optimized at the B3LYP/6-311G(d,p), MP2 energies for the *cis–cis* structure are ∼1.58–1.84 kcal/mol higher relative to the *cis–trans*; however, it shows to be more stable than the *trans–trans* structure. Overstabilization of the *cis–cis* structures is even more evident for geometries optimized at the MP2 level, where the *cis–cis* structures are only higher in energy by ∼0.2–0.5 kcal/mol relative to the *cis–trans* structures. MP2 stacking interaction energies have been shown to be larger than the CCSD(T) methods at the same basis set, although there is no systematic trend in the shifts.[41,42] For some systems, basis set superposition errors are evident in MP2 relative conformational energies.[43−45] Further, gas-phase IR spectroscopy of compound **1** did not show the presence of the *cis–cis* structures since they are the higher energy, minimally populated conformation.[14] Therefore, we carried out another set of calculations where counterpoise corrections to BSSE are incorporated in the geometry optimizations at the MP2 level (data not shown in Table 1). The relative energies of the *cis–cis* conformer changes to 3.1 kcal/mol [MP2/6-311G(d,p)] and 2.6 kcal/mol [MP2/6-311G(2d,p)], consistent with experimentally derived relative stabilities of the equilibrium conformers.[14] Additionally, B97D methods predict approximately small differences in the relative energies across the various basis sets used. It also predicts the relative stabilities of the conformations as reported from experiment with the *cis–trans* as the most stable and *cis–cis* as the least stable. At B97D, the *cis–trans* conformer is predicted to be ∼1.2–1.7 kcal/mol more stable than the *trans–trans* conformer, while the *cis–cis* conformer has energies ranging from ∼1.2 to 2.5 kcal/mol. The inclusion of diffuse functions in the basis sets tends to stabilize the *cis–cis* conformer more at the B97D level. Benchmarking

dx.doi.org/10.1021/jp503539m | J. Phys. Chem. A 2014, 118, 5304–5315

Table 1. Relative Energies of Conformations of *N,N′*-Diphenylurea (kcal/mol)

	relative energies (kcal/mol)[a]								
	A[b]			B[b]			C[b]		
level of theory	T−T	C−T	C−C	T−T	C−T	C−C	T−T	C−T	C−C
B3LYP/6-311G(d,p)	0.116	0.000	5.163	0.000	0.387	7.823	0.116	0.000	5.163
B3LYP/6-311G(2d,p)	0.222	0.000	5.105	0.000	0.134	7.801	0.248	0.000	5.114
B3LYP/6-311+G(d,p)	0.168	0.000	4.501	0.000	0.288	7.092	0.138	0.000	4.516
B3LYP/6-311+G(2d,p)	0.639	0.000	4.479	0.000	0.083	7.047	0.170	0.000	4.404
MP2/6-311G(d,p)	2.059	0.000	1.580	2.415	0.000	0.147	2.477	0.000	0.160
MP2/6-311G(2d,p)	1.849	0.000	1.838	2.259	0.000	0.399	2.259	0.000	0.399
B97D/6-311G(d,p)	1.240	0.000	2.391	1.047	0.000	2.268	1.646	0.000	2.038
B97D/6-311G(2d,p)	1.473	0.000	2.351	1.215	0.000	2.482	1.718	0.000	2.101
B97D/6-311+G(2d,p)	1.519	0.000	1.720	1.341	0.000	1.722	1.746	0.000	1.361
B97D/tzvp	1.519	0.000	2.034	1.185	0.000	2.035	1.732	0.000	1.710

[a]For each set, the minimum energy conformation at each level is used as the reference: T−T, *trans*−*trans*; C−T, *cis*−*trans*; C−C, *cis*−*cis*. [b]A, single-point energies based on B3LYP/6-311G(d,p) geometry; B, single-point energies based on MP2/6-311G(2d,p) geometry; C, full optimization at each level of theory.

Table 2. Relative Energies of Conformations of *N,N′*-Dimethyl-*N,N′*-diphenylurea (kcal/mol)

	relative energies (kcal/mol)[a]								
	A[b]			B[b]			C[b]		
level of theory	T−T	C−T	C−C	T−T	C−T	C−C	T−T	C−T	C−C
B3LYP/6-311G(d,p)	4.488	1.117	0.000	2.591	0.000	1.164	4.489	1.117	0.000
B3LYP/6-311G(2d,p)	4.505	1.216	0.000	2.477	0.000	1.281	4.490	1.208	0.000
B3LYP/6-311+G(d,p)	5.063	1.578	0.000	2.637	0.000	0.970	4.671	1.605	0.000
B3LYP/6-311+G(2d,p)	5.029	1.622	0.000	2.529	0.000	1.041	4.953	1.611	0.000
MP2/6-311G(d,p)	9.636	3.811	0.000	11.793	5.462	0.000	11.970	5.453	0.000
MP2/6-311G(2d,p)	9.219	3.729	0.000	11.614	5.558	0.000	12.507	5.558	0.000
B97D/6-311G(d,p)	6.224	2.182	0.000	6.447	2.312	0.000	6.722	2.439	0.000
B97D/6-311G(2d,p)	6.169	2.249	0.000	6.134	2.164	0.000	6.586	2.454	0.000
B97D/6-311+G(2d,p)	6.721	2.690	0.000	6.477	2.458	0.000	6.963	2.849	0.000
B97D/tzvp	6.519	2.503	0.000	6.206	2.192	0.000	6.750	2.621	0.000

[a]For each set, the minimum energy conformation at each level is used as the reference: T−T, *trans*−*trans*: C−T, *cis*−*trans*; C−C, *cis*−*cis*. [b]A, single-point energies based on B3LYP/6-311G(d,p) geometry; B, single-point energies based on MP2/6-311G(2d,p) geometry; C, full optimization at each level of theory.

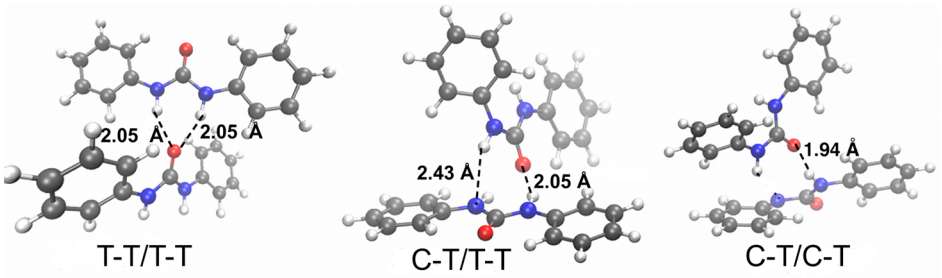

Figure 4. Representative optimized model dimer structures which illustrate the existence of H-bonding interaction in compound **1** (T−T, *trans*−*trans*; C−T, *cis*−*trans*).

studies[46−48] of several other compounds have shown that B97D[49] method and other density functional methods including PBE, BP86, and MO6-2X give accurate estimates of torsional energies and intermolecular interactions.

The differences in the energies between the conformations can be attributed to the interplay among various interactions. The planar *trans*−*trans* structure is stabilized mainly by delocalization interactions between the aromatic group and the urea group such as nonbonding orbitals of the urea nitrogen to π^* orbitals of the ring ($n_{\text{urea N}} \rightarrow \pi^*_{\text{ring}}$). However, this stabilizing interaction in the *trans*−*trans* structure is compensated for by steric interactions between the π orbitals of the aromatic ring and the lone pair of the urea nitrogen, and a weak steric interaction of the two lone pairs of the urea nitrogens. In addition, there are weak delocalization interactions that favor the *cis*−*trans* structure, specifically $\sigma_{\text{NH}} \rightarrow \pi^*_{\text{ring}}$ (closest C−C bond to the N−H group) and $\pi \rightarrow \sigma^*_{\text{NH}}$ between the *trans*-amide group and the opposing aromatic ring. This interaction was also pointed out previously[14] as the stabilizing interaction of the *cis*−*trans* conformer. Although the *cis*−*cis* structure is weakly stabilized by a nonoptimal displaced parallel π-stacking interaction between the two rings, it has the highest energy due

dx.doi.org/10.1021/jp503539m | J. Phys. Chem. A 2014, 118, 5304−5315

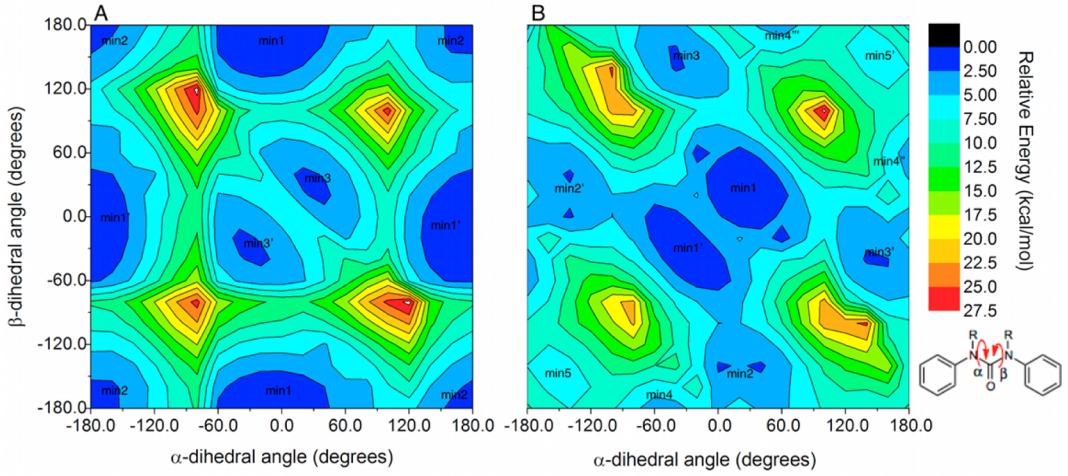

Figure 5. Two-dimensional energy profiles for rotation around the α- and β-dihedral angles of compounds **1** (A) and **2** (B).

to the loss of the delocalization energy between the aromatic rings and the urea group. Further, destabilizing steric interactions between the carbonyl and amide groups are more predominant in this conformation, with a N−H to C═O distance of 2.36 Å. Previous theoretical gas-phase optimizations[14,15] at the B3LYP/6-31G(d,p) level of compound **1** also showed the *cis*−*trans* conformation to be the most stable and close in energy to the *trans*−*trans* conformation. However, the crystal structure of **1** shows *trans*−*trans* to be the predominant conformation,[50,51] which is stabilized mainly by intermolecular N−H···O H-bond interaction.[50] The oxygen atom of the carbonyl group is responsible for the existence of two N−H···O intermolecular interactions. The calculated difference in energy between the *cis*−*trans* and *trans*−*trans* conformations is very close, supporting the existence of both conformers in both states.

We also optimized model dimer structures of compound **1** with varying conformations at the B97D/6-311G(d,p) level of theory to illustrate possible intermolecular interactions. Representative optimized structures of the probable dimers are presented in Figure 4. From the optimized dimer structures, it is evident that intermolecular H-bonding interactions are existent in multimolecule samples, such as the solid state. The model dimer structures show intermolecular N−H···O and N−H···N interactions. From the set of model structures generated, the most stable configurations correspond to a *cis*−*trans*/*trans*−*trans* dimer. Based on these results, we can deduce from the calculated probable dimer configurations that H-bonding is also a predominant interaction in the solid matrix and further supports the existence of both *cis*−*trans* and *trans*−*trans* conformations. IR data and frequency calculations also support this argument (discussed below).

In the case of compound **2**, the *cis*−*cis* conformation has the lowest energy among the conformations as predicted at different levels of theory and basis sets (Table 2) with the exception of B3LYP energies generated from MP2-optimized geometries. The *cis*−*trans* conformation has slightly higher energy, predicted to be ∼1.2−2.8 kcal/mol relative to the *cis*−*cis* using B3LYP and B97D at various basis sets, while a much higher energy difference is calculated at the MP2 level at ∼3.7−5.6 kcal/mol. The *trans*−*trans* is shown to be the highest energy conformation, which is calculated to be ∼4.5−5.0 kcal/mol relative to the *cis*−*cis* at the B3LYP level of theory and 6.2−7.0 kcal/mol at B97D. At the MP2 level, this conformation is shown to be ∼9.2−11.8 kcal/mol higher in energy than the *cis*−*cis* conformation. Although there are discrepancies in the calculated energies at the different levels of theory, the relative stability of the conformers is consistent with previously observed behavior of this compound.[11,12,19,52] Previous studies predict the relative energies of the *cis*−*cis* (endo) and *cis*−*trans* (exo) conformations extrapolated from the high-level ab initio approach with higher order correlation effects (CCSD(T)) to be approximately 3.2 kcal/mol.[18] Among the methods used, the MP2 methods predict more comparable relative energies with previously calculated energies from the CCSD(T) method.[18] However, B97D also gave values that are almost equivalent to the high-level CCSD(T) method[18] with ∼0.35 kcal/mol differences in energies.

The difference in the preferential conformation of compound **2** relative to compound **1** is due to an average effect of various interactions present within the molecule. In compound **2**, the *cis*−*cis* conformation is stabilized by a displaced parallel π-stacking interaction. The distance between the center of mass of the two phenyl rings is approximately 4.13 Å in the *cis*−*cis* structure. In addition, our analysis shows that the lone pair electrons of the urea nitrogen atoms are involved in delocalization interactions between the aromatic ring and the urea group, and the stabilization is more predominant in the *cis*−*cis* conformation as opposed to the *cis*−*trans* and *trans*−*trans* conformations. Steric analysis also reveals that one of the predominant factors that favor the folded structure upon addition of the methyl group on the urea nitrogens is due to unfavorable steric interactions present in the *trans*−*trans* and *cis*−*trans* structures. The total pairwise steric exchange energy is lowest in the *cis*−*cis* conformation while it shows the highest value for the *trans*−*trans* structure. As opposed to compound **1**, the *trans*−*trans* structure of compound **2** is nonplanar due to the presence of the bulky methyl groups. Addition of substituents such as methyl or ethyl groups on the amide nitrogens has also been previously shown to induce the folded conformation of *N*,*N*′-diphenylurea.[17−19]

Based on our results, there are observed discrepancies in the calculated relative energies of the conformers at the various levels of theory. However, the B97D method has predicted relative stabilities of the conformers for compounds **1** and **2** consistent with previous experiments.[14,18] Further, B97D is computationally inexpensive but yields relative stabilities of conformers consistent with experimental data. Therefore, in

dx.doi.org/10.1021/jp503539m | J. Phys. Chem. A 2014, 118, 5304−5315

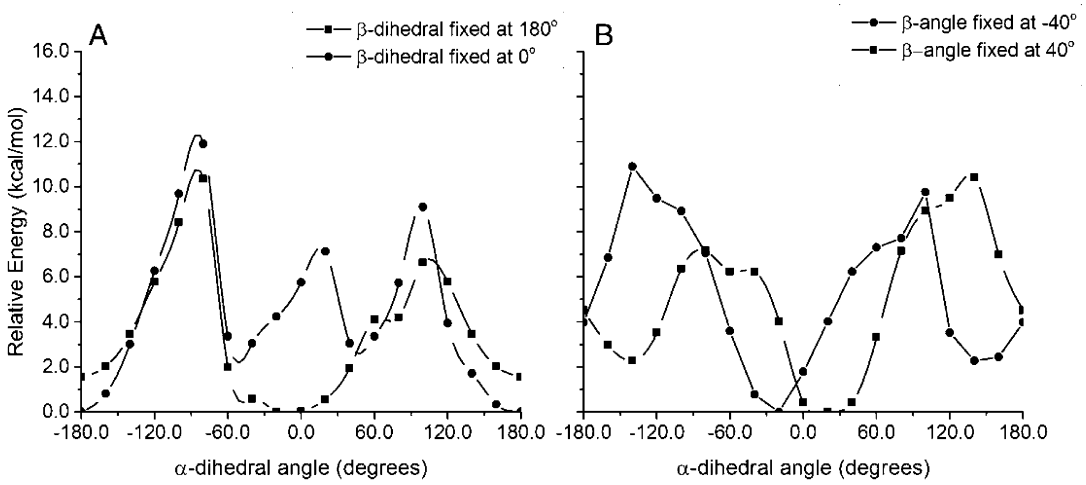

Figure 6. One-dimensional torsional energy profiles of compounds **1** (A) and **2** (B) for rotation around the α-dihedral angle with β-dihedral fixed at 180° or 0° and ±40°, respectively.

determining the 2-D torsional profiles of compounds **1** and **2**, we have carried out calculations at the B97D/6-311G(d,p) level.

3.2. Torsional Energy Profiles. To explore the conformational space of compounds **1** and **2**, we calculated the two-dimensional energy profile for rotation around the urea bonds using the DFT method, B97D/6-311G(d,p). Figure 5A shows the two-dimensional torsional potential energy profile of compound **1**. As shown in Figure 5, there are three types of minima with respect to the α- and β-dihedral angles (labeled as min1, min2, and min3 and the symmetrical energy wells labeled as min1′, min2′, and min3′). Min1 corresponds to the *cis*−*trans* conformation of the compound with respect to the amide group while min2 corresponds to the extended *trans*−*trans* conformation. At the B97D/6-311G(d,p) level of theory, the folded *cis*−*trans* conformation (±20°, 180°; 0°, 180° are very close in energy, ∼0.0055 kcal/mol) is the global minimum but only slightly more stable (∼1.6 kcal/mol) than the extended *trans*−*trans* (180°,180°).

The *trans*−*trans* conformation is planar and stabilized mainly by the π-electron delocalization between the phenyl rings and the urea group. At 180°, 180°, the extended structure allows for π-electron delocalization between the aromatic rings and the urea group. Looking at the slice with the β-dihedral angle fixed at ±180°, the energy increases as the urea group is rotated out of plane and corresponds to a barrier of ∼10.3 kcal/mol at around −80°. The increase in energy as the α-conformation changes from −180° to −80° is partly due to the loss of the stabilizing π-electron delocalization (Figure 6A). At 0°, the energy is at a minimum (min1) and the energy rises as the dihedral angle is rotated in the positive direction traversing a barrier of ∼6.6 kcal/mol to a *trans*−*trans* structure (±180, ±180). Starting from the global minimum conformation at 180°, 0° (min1′; β-dihedral angle fixed at 0°), it requires an energy barrier of ∼11.9 kcal/mol to cross to the potential well around min3′. Min3 and min3′ (±20° to ±40°) correspond to minimum energy conformers where the two phenyl rings of *N*,*N*′-diphenylurea are folded in a *cis*−*cis* conformation but are approximately 2.6 kcal/mol higher in energy from the global minimum.

Figure 5B shows the two-dimensional potential energy profile for rotation of C_{urea}−N_{urea} bonds in compound **2**. The global minima are labeled as min1 and min1′, which correspond to the folded *cis*−*cis* structure with respect to the amide bond where the phenyl rings are in a stacked orientation. The global minimum in this potential energy surface is at ±40°, ±20° conformation. As discussed above, the folded structure is stabilized by weak π-stacking interaction between the two phenyl rings and has minimal steric interaction as opposed to the extended conformation. From the conformation at min1 (40°, 20°), it requires a maximum of 7.2 kcal/mol to traverse to the *cis*−*trans* conformation at −180°, 40° in one *trans*ition path (Figure 6B). Approximately 9.8 kcal/mol is required on another *trans*ition path (−40°, −20° to 40°, 180°). The minimum energy *trans*ition from *cis*−*cis* to a *cis*−*trans* conformation requires a barrier of 5.1 kcal/mol. The differences in energies with rotation of the urea bond in several directions can be attributed to the orientation of the methyl groups with respect to the urea group as the rotations occur (+ or − direction). The min2, min2′; min3, min3′; and min4, min4′, min4″, min4‴ are the minima corresponding to *cis*−*trans* conformations. Min5 and min5′ correspond to the extended conformation but not completely planar at either ±140° or ±160°. The *trans*−*trans* conformations are ∼6.5 kcal/mol higher than the global minimum.

In summary, the two-dimensional profiles provide information on the conformational space and the energetically favorable conformations of compounds **1** and **2**. The 2-D profiles clearly show the change in conformational preference upon adding a methyl substituent on the urea nitrogen atoms. For compound **1**, *cis*−*trans* (α = 0°, β = 180°, or vice versa), *trans*−*trans* (α = 180°, β = 180°) and *cis*−*cis* (α = ±20°, β = ±40° or α = ±40°, β = ±20°) are identified as the minimum energy conformers with the *cis*−*trans* and *trans*−*trans* conformers as the energetically favored ones. Similarly, for compound **2**, *cis*−*cis* (α = ± 40°, β = ±20°, or vice versa) conformers are energetically favored while the *trans*−*trans* conformers are less energetically favored. The profiles also provide information on the amount of energy required to convert from one conformation to another.

3.3. IR Spectroscopy. We carried out infrared spectroscopy of compounds **1** and **2** in solid state and DMSO solution to determine the population of conformers by probing the fundamental vibrations that are sensitive to conformational change and exhibit structure in the spectra. We also performed vibrational frequency calculations of compounds **1** and **2** to aid

dx.doi.org/10.1021/jp503539m | J. Phys. Chem. A 2014, 118, 5304−5315

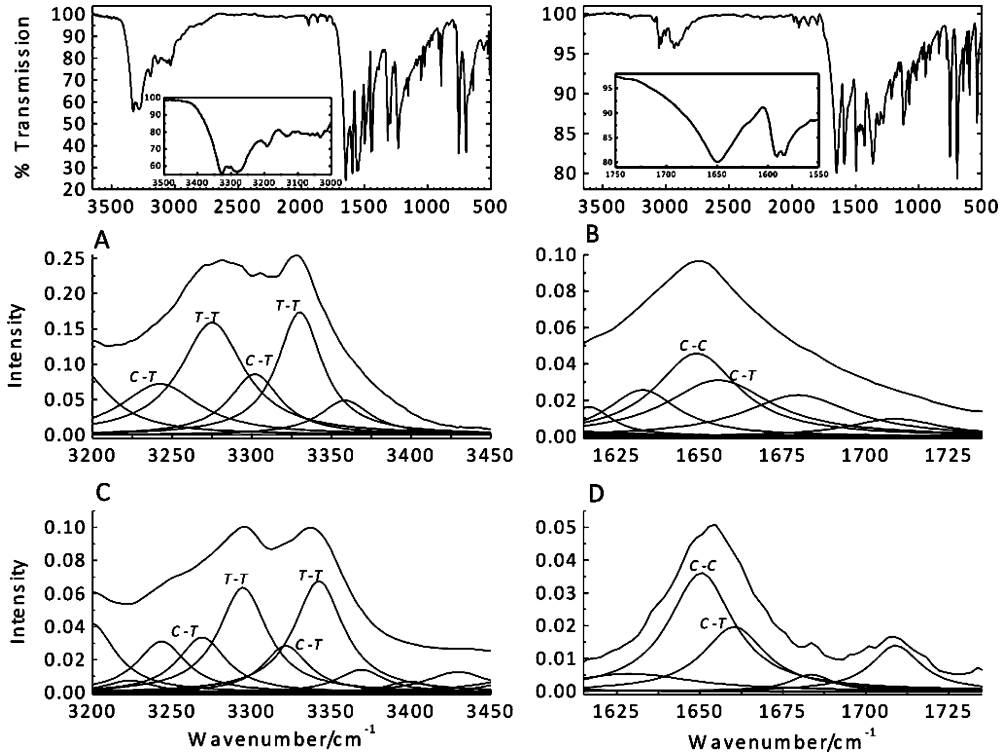

Figure 7. FTIR spectra of *N,N′*-diphenylurea, **1** (top left) and *N,N′*-dimethyl-*N,N′*-diphenylurea, **2** (top right) in the solid matrix. The insets show the N−H stretching and C═O stretching modes, which are used to calculate the relative populations of conformers for compounds **1** and **2**, respectively, using a Lorentzian function (spectra A−D). The Lorentzian fits of the IR spectra in the solid matrix (A and B) and in DMSO solvent (C and D) are shown.

Table 3. Assignment of Vibrational Frequencies (cm^{-1}) of Selected Normal Modes of *N,N′*-Diphenylurea and *N,N′*-Dimethyl-*N,N′*-diphenylurea in KBr Matrix and DMSO Solvent

	N,N′-diphenylurea[a]			*N,N′*-dimethyl-*N,N′*-diphenylurea[a]		
	calcd freq[c] (cm^{-1})					
exptl freq[b] (cm^{-1})	monomer	dimer[d]	assignment	exptl freq[a] (cm^{-1})	calcd freq[b] (cm^{-1})	assignment
3330/3342	3509	3405	T−T N−H sym str		1691	T−T C═O str
3302/3321	3504	3443	C−T N−H str (*cis* to C═O)	1656/1660	1675	C−T C═O str
				1649/1650	1674	C−C C═O str
3275/3294	3495	3381	T−T N−H asym str			
3242/3269	3487	3366	C−T N−H str (*trans* to C═O)			

[a]Complete list and assignment of the experimental vibrations are shown in Supporting Information Tables S3 and S4. [b]The frequency of the modes in the solid matrix/solution are noted in this order. [c]Scaling factor = 0.968. [d]The calculated frequencies are based on the most stable model dimer structures. The frequencies shown are only H-bonded N−H stretches. N−H modes that do not exhibit H-bonding have frequencies very similar to the monomer units.

in the assignment of their normal modes and experimental frequencies. The reported theoretical vibrational frequencies were obtained at the B3LYP/6-311G(d,p) level of theory, which has been shown to yield frequencies that are usually in excellent agreement with experimental frequencies in conjunction with the appropriate scaling factor.[29,53] To estimate conformer populations, the IR spectra of **1** and **2** are best fit to the sum of Lorentzian curves from two conformers.[54] The main bands were fit and assigned to the most stable conformer, while the shoulders and weaker features were assigned to the less energetically stable species which demonstrate strong enough dipole moments to be detected in certain regions. The presence of two conformations is further supported by the low-energy barriers to rotation between the two more stable conformers in **1** and **2**, as described previously.

In the case of compound **1**, the N−H stretching modes (3240−3330 cm^{-1}) are sensitive to conformational changes between the *trans*−*trans* to *cis*−*trans* form. For each N−H stretching mode, a difference of approximately 25−40 cm^{-1} between the two conformations is obtained based on Lorentzian fitting (Figure 7). At slightly lower energy in the 3030−3190 cm^{-1} region, weaker features corresponding to phenyl ring C−H stretching vibrations occur predominantly due to the presence of the *trans*−*trans* conformation. At lower energy, a prominent C═O stretching vibration is observed at 1648 cm^{-1} due to *trans*−*trans*, although there may be some overlap of this mode with the *cis*−*trans* form, as suggested by the theoretical calculations. Within this region, several very intense bands occur at 1594, 1560, 1498, 1448, 1440, 1315, and 1221 cm^{-1}, all peaks of which are ascribed to the *trans*−*trans* conformer, and some of which show subtle shoulders that are

dx.doi.org/10.1021/jp503539m | J. Phys. Chem. A 2014, 118, 5304−5315

attributed to the *cis*−*trans* form. These peaks are assigned to N−H bending and ring in-plane deformations and a mix of these modes. Further into the IR, the 500−1000 cm^{-1} region is dominated by in-plane and out-of-plane wagging modes, with two intense peaks at 753 and 697 cm^{-1}. A detailed list of the vibrational modes and their corresponding frequencies are listed in SI Table S3.

From our set of model dimer structures, we calculated IR frequencies of the most stable dimer configuration. Vibrational analyses of the most stable dimer structure of compound **1** show that the scaled H-bonded N−H stretching frequencies are in close agreement with the experimental frequencies compared to the N−H stretching frequencies in the monomer or non-H-bonded N−H in the dimer structures (not shown in Table 3 but very close in frequencies to the monomer normal modes). Our calculations show that H-bonded amide N−H stretching frequencies are downshifted compared to the non-H-bonded frequencies. These results further support the existence of extensive hydrogen bonding in the solid structure. Previous studies have also shown that H-bonding causes shifts in the N−H stretch vibration depending on the molecular environment.[55,56] In most cases, H-bonding causes a red shift in the N−H stretching frequencies. In DMSO solution, there is an observed ∼20 cm^{-1} blue shift in the N−H frequency relative to the solid-state spectra. This result suggests that the extensive H-bonding interaction in the solid matrix has been disrupted by the solvent. Although compound **1** exhibits H-bonding interaction with DMSO (as it is a strong H-bonding acceptor), the intermolecular interactions present are not as strong as in the solid structure, hence, the blue shift in the N−H stretching frequency. Stronger intermolecular forces in the solid structure can be attributed to its compact nature while the intermolecular hydrogen bonds are much more dynamic in DMSO.

Addition of methyl groups on the *N*,*N*′ positions as in the case of *N*,*N*′-dimethyl-*N*,*N*′-diphenylurea slightly complicates the IR spectrum due to the extra vibrational modes arising from the methyl C−H stretches (Figure 7). In the higher energy region, a group of medium weak bands is assigned to the aromatic C−H stretching (2960−3080 cm^{-1}) and methyl C−H stretching (2820−2935 cm^{-1}) modes, mostly due to the presence of the *cis*−*cis* conformer. At lower energy, several intense bands are observed, namely, at 1649, 1593, 1584, 1496, and 1365 cm^{-1}. The 1649 cm^{-1} band is assigned to a C═O stretching vibration mixed with methyl C−H wags and ring in-plane stretching deformations. Our theoretical normal-mode analysis of the different conformers demonstrates that the C═O stretching mode occurs very close in frequency for the *cis*−*cis* and *cis*−*trans* conformers. Our simulations indicate that the best fit to this band can be obtained by incorporating a weak Lorentzian feature ∼7 cm^{-1} (*cis*−*trans*) at higher energy relative to the main band (*cis*−*cis*), the trend of which is consistent with theoretical predictions. The two-peak feature at 1593 and 1584 cm^{-1} arises from ring in-plane stretching deformations and minor contributions from methyl C−H wags and a C═O stretch. A shoulder at 1633 cm^{-1} is assigned to the less stable *cis*−*trans* conformer having the same motion as its *cis*−*cis* counterpart. The band at 1496 cm^{-1} has mixed vibrations from a *cis*−*cis* ring in-plane stretching deformation, methyl C−H *scissoring*/wags, and ring-N symmetrical stretches. At lower energy, the intense band at 1365 cm^{-1} is associated with a ring C−H in-plane bend coupled with a N−(C═O)−N antisymmetric stretching mode. Further into the IR spectrum, two intense bands at 753 and 697 cm^{-1} are apparent, which like its unmethylated counterpart, are attributed to C−H wagging modes of the more stable conformer. Throughout the lower energy region (500−1000 cm^{-1}), bands arise from motions related to the phenyl ring, such as ring-CH wags, ring in- and out-of-phase breathing, ring in-plane bending deformation, and ring tilting. A detailed list of the vibrational modes and their corresponding experimental and theoretical frequencies are shown in SI Table S4. For both samples, condensed summaries of select vibrational frequencies are presented in Table 3.

In DMSO solution, only very slight shifts in the C═O stretching frequencies are observed relative to the solid-state spectra. Trajectory analysis of MD simulation of compound **2** in DMSO (discussed later in detail) exemplifies possible dipole interaction between the slightly positive $C_{carbonyl}$ atom of **2** and DMSO. However, the electronic nature of the compound suggests these interactions are very weak, hence barely affecting the C═O stretching frequencies.

3.4. NMR Spectroscopy. Figure 8 shows the ^1H NMR spectrum of compound **1** in $CDCl_3$ and displays chemical shifts

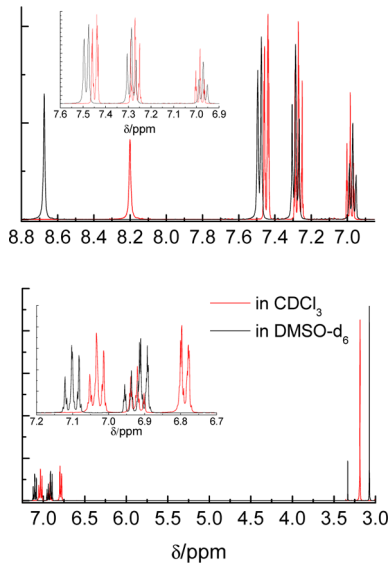

Figure 8. NMR spectra of *N*.*N*′-diphenylurea, **1** (top), and *N*,*N*′-dimethyl-*N*,*N*′-diphenylurea, **2** (bottom), in $CDCl_3$ (red lines) and DMSO-d_6 (black lines). The chemical shift occurring at 3.4 ppm in the NMR spectrum of **2** in DMSO arises from water contamination.

at 8.20 δ (singlet), 7.45 δ (doublet), 7.27 δ (triplet), and 6.99 δ (triplet). These peaks are assigned to N−H, and the aromatic ortho-, meta-, and para-H, respectively. The spectrum indicates the presence of a symmetrical molecule, most likely the *trans*−*trans* conformer. In this case, the phenyl proton chemical shifts are expected to be different between an aromatic ring *trans* to the C═O group (or C═S, which has comparable magnetic anisotropy) and that of a *cis* conformation.[57] For example, the aromatic para-H in *N*,*N*′-arylalkylureas[52] or *N*,*N*′-arylalkylthioureas[57] whose phenyl group is *trans* to the C═O/C═S group typically has a resonance at ∼6.95−6.99 δ, while that of the *cis* conformer occurs more downfield. Comparison of our NMR spectrum with these previous studies denotes that compound **1** in $CDCl_3$ exists predominantly as a *trans*−*trans* conformer. These results are consistent with the theoretically calculated population in $CDCl_3$ (see below). In DMSO-d_6, the ^1H NMR spectrum of compound **1** displays comparable

dx.doi.org/10.1021/jp503539m | J. Phys. Chem. A 2014, 118, 5304−5315

Table 4. Percentages of Conformations of *N,N′*-Diphenylurea and *N,N′*-Dimethyl-*N,N′*-diphenylurea in Different Environments Calculated from MD Simulations

	N,N′-diphenylurea			*N,N′*-dimethyl-*N,N′*-diphenylurea		
environment	*trans*−*trans*	*cis*−*trans*	*cis*−*cis*	*trans*−*trans*	*cis*−*trans*	*cis*−*cis*
Boltzmann estimate	5.8	91.2	3.0	0.0	1.6	98.4
gas (MD)	9.8	90.0	0.2	0.0	2.6	97.4
chloroform (MD)	98.1	1.9	0.0	1.5	24.0	74.4
DMSO (MD)	99.7	0.3	0.0	6.4	39.3	54.3

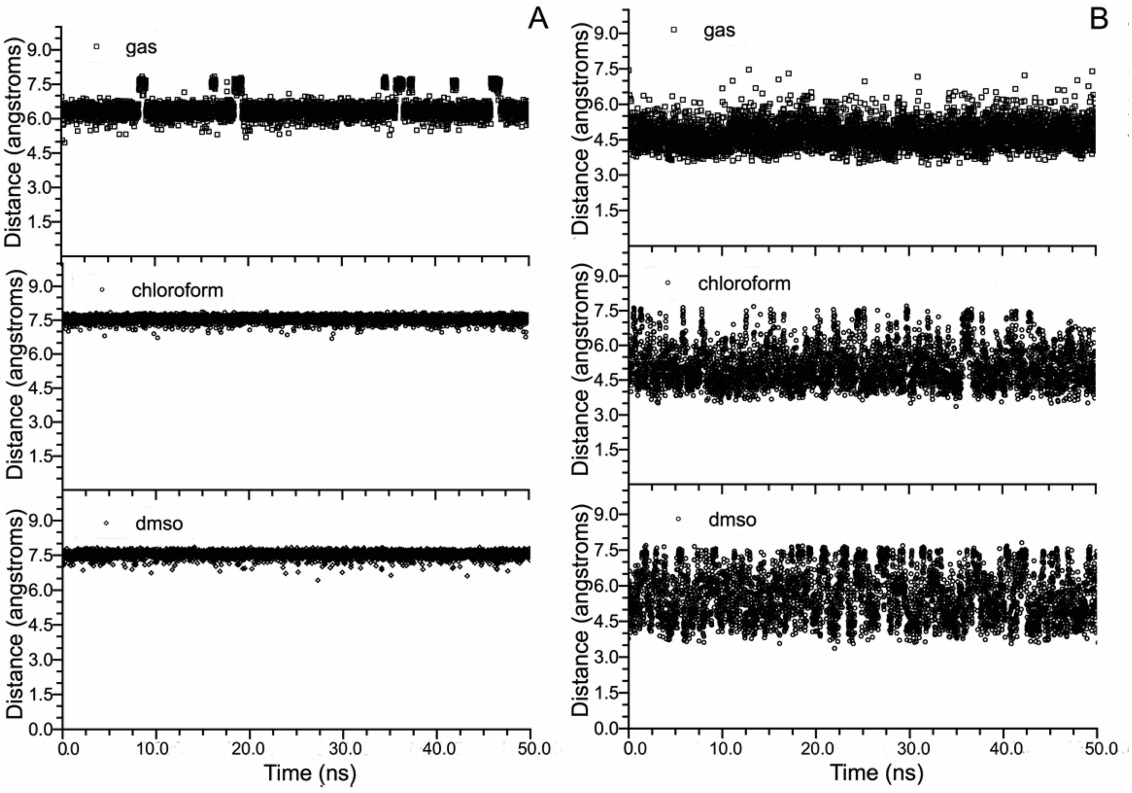

Figure 9. Change in distance between the center of mass of the phenyl rings of compounds **1** (A) and **2** (B) throughout the 50 ns simulation.

chemical shifts, except that the singlet is shifted 0.45 ppm downfield compared to that in $CDCl_3$. Here, a singlet at 8.68 δ, a doublet at 7.48 δ, and two triplets at 7.28 δ and 6.97 δ are observed, which have similar proton assignments to that in $CDCl_3$. The downfield shift in the N−H resonance may arise from the interaction of DMSO-d_6 with compound **1**, thus deshielding the proton and shifting its resonance to higher frequency. This may occur either through an H-bonding interaction between $O_{DMSO}\cdots H-N_{urea}$ or dipole−dipole interaction between $O_{DMSO}\cdots C{=}O_{urea}$, thus pulling away electron density from the protons in N−H. Given the similar spectral features of the ^{1}H peaks in $CDCl_3$ and DMSO-d_6, it is likely that compound **1** also exists as a *trans*−*trans* conformer in the aprotic solvent. This idea is consistent with MD simulations in DMSO (see below).

The ^{1}H NMR spectrum of compound **2** in $CDCl_3$ displays chemical shifts at 7.03 δ (triplet), 6.93 δ (triplet), 6.80 δ (doublet), and 3.19 δ (singlet) (Figure 8). These multiplet peaks are assigned to the aromatic meta-, para-, and ortho-protons, respectively, while the singlet corresponds to the methyl protons. The aromatic proton resonances in our work are consistent with a previous study which demonstrates that an upfield shift is observed as a result of the presence of another phenyl ring on the second nitrogen.[58] The chemical shift can be justified if the protons are oriented close to one another by having the two aromatic rings lie above each in a folded geometry, thereby inducing a ring current upfield shift. In $CDCl_3$, the *cis*−*cis* conformation of compound **2** is therefore predominant, which is consistent with our MD simulations (see below). Changing the environment from a nonpolar to an aprotic solvent such as DMSO-d_6 produces a ^{1}H NMR spectrum with chemical shifts occurring at 7.10 δ (triplet), 6.91 δ (multiplet), and 3.07 δ (singlet). The group of peaks at 6.91 δ arises from a doublet and triplet (both of which are more clearly separated in $CDCl_3$) coalescing into a multiplet which suggests strong coupling between the ortho- and para-protons in the presence of DMSO-d_6. Compared to the proton resonances in $CDCl_3$, the chemical shifts in DMSO-d_6 are collectively shifted downfield, analogous to the trend observed in compound **1**. Here, DMSO-d_6 presumably interacts with the carbonyl group of **2**, thus shifting electron density away from the aromatic protons, and induces a deshielding effect. On the other hand, the interaction of the solvent with the molecule induces a shielding effect on the methyl protons as evidenced by a slight upfield shift. Similar to that in $CDCl_3$, compound **2** may mainly exist in the folded form as seen from the single

dx.doi.org/10.1021/jp503539m | J. Phys. Chem. A 2014, 118, 5304−5315

methyl proton peak arising from the symmetric *cis*–*cis* conformer.

3.5. Conformational Behavior in Different Environments. We carried out MD simulations and IR and NMR spectroscopies to determine the conformational preferences and dynamic behavior of compounds **1** and **2** in different environments. To determine the conformations of compounds **1** and **2** from the trajectories obtained from MD simulations, we defined α- and β-dihedral angles, which correspond to $C_{aromatic}$–N_{urea}–C_{urea}–$O_{carbonyl}$ dihedral angle. *Trans* conformations have dihedral angle values within the ±60° window, and those outside are defined as *cis* conformations. Dynamic behavior of the conformations was determined by calculating the distance between the center of mass of the two phenyl rings in compounds **1** and **2**. Shorter distances indicate the presence of the folded conformations.

For compound **1** in gas phase, the calculated relative populations are ∼90.0% of *cis*–*trans*, ∼9.8% *trans*–*trans*, and 0.2% *cis*–*cis* conformers (Table 4). The fractional population is consistent with the calculated relative energies of the conformers for **1**. The conformations are also estimated using the Boltzmann equation using the B97D/6-311G(d,p) energies from Table 1 (Boltzmann estimate of populations calculated using energies at different levels of theory are shown in SI section 3). As shown in Table 4, from the Boltzmann relationship, the calculated populations are ∼91.2% *cis*–*trans*, ∼5.8% *trans*–*trans* and 3.0% *cis*–*cis*. Gas-phase spectroscopy of compound **1**[14] showed the *cis*–*trans* conformer to be predominant over the *trans*–*trans* form, while the *cis*–*cis* one was not observed. Crystal structures, however, demonstrate the presence of the *trans*–*trans* conformation, most likely stabilized by intermolecular hydrogen bonding interaction in the crystal.[50] Based on the calculations discussed previously and the model dimer structures, we deduce the presence of both *trans*–*trans* and *cis*–*trans* conformations in the solid matrix. The experimentally determined contributions in solid state are roughly estimated at 88 ± 2% *trans*–*trans* and 12 ± 1% another conformer of **1**, which we predict to be *cis*–*trans*.

In chloroform and DMSO, MD simulations indicate that compound **1** has *trans*–*trans* as the dominant conformation, at 98.1% and 99.7%, respectively. NMR results in chloroform and DMSO show predominance of a symmetrical molecule (see prior section), which our MD simulations demonstrate as the *trans*–*trans* conformation. Using IR spectroscopy, population analysis of **1** in DMSO indicates 88 ± 4% of the dominant *trans*–*trans* conformer and a smaller contribution at 12 ± 1% for the minor component, which is the *cis*–*trans* form. Although there is ∼10% discrepancy in the relative populations derived from MD simulations and IR spectroscopy, in general, the presence of solvent tends to stabilize the extended *trans*–*trans* conformation as opposed to the *cis*–*trans* conformation in the gas phase. In the polar aprotic solvent DMSO, compound **1** exhibits H-bonding interaction with the solvent, O_{DMSO}···H–N_{urea}, stabilizing the extended all-*trans* conformation. Figure 9A shows the distance between the center of mass of the two phenyl rings of compound **1** in gas, chloroform, and DMSO throughout the 50 ns simulation. In gas phase, compound **1** remains predominantly *cis*–*trans* but fluctuates to the *trans*–*trans* conformations. The distances are fluctuating between 4.39 and 7.9 Å with an average distance of 6.4 Å. In chloroform and DMSO, compound **1** is predominantly in the *trans*–*trans* structure with the distances fluctuating between 6.3 and 7.9 Å (mean = 7.5 Å) and 5.9–8.0 Å (mean = 7.5 Å), respectively.

Addition of methyl groups at the *N*,*N*′- positions changes the energetics of the conformations and therefore influences the population of the conformers present for **2**. From the gas-phase MD simulation, the folded *cis*–*cis* conformation is preferentially stabilized over the *cis*–*trans* conformer, with 97.4% *cis*–*cis* and only 2.6% *cis*–*trans*. This distribution is consistent with the relative populations calculated using the Boltzmann equation with 98.4% *cis*–*cis* and 1.6% *cis*–*trans*. The Boltzmann estimates shown in Table 4 are derived from energies calculated at B97D/6-311G(d,p). Populations derived from energies obtained at different basis sets are shown in the Supporting Information. The gas-phase populations are consistent with relative stabilities of the conformers calculated previously. The contributions in the solid matrix are estimated at 67 ± 3% of the dominant conformer (presumably *cis*–*cis*) and 33 ± 1% of the less stable form (most likely *cis*–*trans*) (Figure 7). As demonstrated through MD simulations, the population still tends to favor the *cis*–*cis* conformer in solution, but to a lower extent. For example, the contributions in chloroform are 74.4% *cis*–*cis*, 24% *cis*–*trans*, and 1.5% *trans*–*trans*. This distribution is more skewed in DMSO, as exhibited by the presence of 54.3% *cis*–*cis*, 39.3% *cis*–*trans*, and 6.4% *trans*–*trans* conformers of compound **2**. In the experimental data, the NMR spectrum suggests the dominant presence of the *cis*–*cis* isomer in chloroform and DMSO. On the other hand, the solution IR spectrum in DMSO reveals a major contribution from one conformer, with lesser amounts of another. For example, Lorentzian fits indicate 71 ± 8% of the dominant conformer (*cis*–*cis*) and 29 ± 3% of the less stable form (*cis*–*trans*). While both experimental and theoretical data do not exactly agree on the absolute contributions of the conformers in **2**, the relative trends are similar. Figure 9B shows the dynamic behavior of compound **2**. In gas phase, the distance between phenyl rings of compound **2** changes from 3.2 to 7.6 Å, with the majority of the conformers existing in the folded conformation. In chloroform and DMSO, the fluctuations among the conformations are much greater compared to gas phase. The variance of the distances is 0.26, 0.73, and 1.04 Å in gas, chloroform, and DMSO, respectively. Figure 9 also demonstrates the dynamic behavior of compound **2**, fluctuating among all stable conformations while compound **1** more or less maintains a single conformation even in solution.

Our results show quantitative analysis of the conformational propensities and dynamic behavior of compounds **1** and **2** in different environments, which allow us to quantify the effect of adding methyl substituents on the urea nitrogens and modifying the environment surrounding these molecules.

4. CONCLUSION

In this work, we explored the molecular basis and quantified the conformational propensities of *N*,*N*′-substituted-diphenylurea foldamer building blocks in different environments using quantum calculations, MD simulations, and IR and NMR spectroscopies. Our results show that compound **1** prefers *cis*–*trans* over *trans*–*trans* in the gas phase, with both conformations significantly populated at room temperature as opposed to the *cis*–*cis* conformer. We deduce from our energetic calculations, analysis of dimer structures, and IR results that both the *trans*–*trans* and *cis*–*trans* conformations are present in the solid matrix, stabilized by intermolecular H-bonding interaction. In both chloroform and DMSO solution, compound **1** exists predominantly in the *trans*–*trans* conformation with only very minimal fluctuation in con-

formation. Addition of methyl substituents on the urea nitrogen atoms (compound **2**) shifts the conformational preference to the folded *cis*−*cis* as the most populated, followed by *cis*−*trans* and negligible amounts of the *trans*−*trans* in all environments. However, significant change is observed in the conformational dynamics in the presence of solvent. The conformational variation is even more pronounced in the presence of an aprotic polar solvent, DMSO. Comprehensive structural analyses of the compounds reveal that various interactions drive the conformational propensities of the compounds. Our detailed quantitative analyses of the conformational propensities of the monomer units in various environments provide a basis for the conformational behavior of oligomers that can be built from these units. Further, as part of our long-term efforts to characterize oligourea foldamers, our results also identify appropriate theoretical methods and experimental molecular tools to study this class of compounds.

■ ASSOCIATED CONTENT

Supporting Information

Text describing detailed basis set study of geometrical parameters and accompanying references, figure showing conformers of *N*,*N*′-diphenylurea and *N*,*N*′-dimethyl-*N*,*N*′-diphenylurea, and tables listing selected geometrical parameters, comprehensive vibrational frequencies and normal modes, and populations based on Boltzmann equation using energies from different levels of theory. This material is available free of charge via the Internet at http://pubs.acs.org.

■ AUTHOR INFORMATION

Corresponding Author

*E-mail: galanj@tamug.edu.

Author Contributions

The manuscript was written through contributions of all authors. All authors have given approval to the final version of the manuscript.

Notes

The authors declare no competing financial interest.

■ ACKNOWLEDGMENTS

This study is supported in part by Welch Foundation Grant No. BD-0046. M.G.I.G. and A.P. acknowledge support from Penn State Erie, The Behrend College, for providing startup financial support and a research summer fellowship, respectively.

■ ABBREVIATIONS

HF, Hartree−Fock; DFT, density functional theory; MP2, Møller−Plesset 2; MD, molecular dynamics; IR, infrared; NMR, nuclear magnetic resonance

■ REFERENCES

(1) Gong, B. Hollow Crescents, Helices, and Macrocycles from Enforced Folding and Folding-Assisted Macrocyclization. *Acc. Chem. Res.* **2008**, *41*, 1376−1386.

(2) Li, Z.-T.; Hou, J.-L.; Li, C. Peptide Mimics by Linear Arylamides: A Structural and Functional Diversity Test. *Acc. Chem. Res.* **2008**, *41*, 1343−1353.

(3) Li, Z.-T.; Hou, J.-L.; Li, C.; Yi, H.-P. Shape-Persistent Aromatic Amide Oligomers: New Tools for Supramolecular Chemistry. *Chem. − Asian J.* **2006**, *1*, 766−778.

(4) Huc, I. Aromatic oligoamide foldamers. *Eur. J. Org. Chem.* **2004**, *2004*, 17−29.

(5) Violette, A.; Lancelot, N.; Poschalko, A.; Piotto, M.; Briand, J.-P.; Raya, J.; Elbayed, K.; Bianco, A.; Guichard, G. Exploring Helical Folding of Oligoureas During Chain Elongation by High-Resolution Magic-Angle-Spinning (HRMAS) NMR Spectroscopy. *Chem.—Eur. J.* **2008**, *14*, 3874−3882.

(6) Tanatani, A.; Kagechika, H.; Azumaya, I.; Fukutomi, R.; Ito, Y.; Yamaguchi, K.; Shudo, K. Helical aromatic urea and guanidine. *Tetrahedron Lett.* **1997**, *38*, 4425−4428.

(7) Violette, A.; Averlant-Petit, M. C.; Semetey, V.; Hemmerlin, C.; Casimir, R.; Graff, R.; Marraud, M.; Briand, J.-P.; Rognan, D.; Guichard, G. *N*,*N*′-Linked Oligoureas as Foldamers: Chain Length Requirements for Helix Formation in Protic Solvent Investigated by Circular Dichroism, NMR Spectroscopy, and Molecular Dynamics. *J. Am. Chem. Soc.* **2005**, *127*, 2156−2164.

(8) Zhang, A.; Han, Y.; Yamato, K.; Zeng, X. C.; Gong, B. Aromatic Oligoureas:Enforced Folding and Assisted Cyclization. *Org. Lett.* **2006**, *8*, 803−806.

(9) Wu, B.; Jia, C.; Wang, X.; Li, S.; Huang, X.; Yang, X.-J. Chloride Coordination by Oligoureas: From Mononuclear Crescents to Dinuclear Foldamers. *Org. Lett.* **2012**, *14*, 684−687.

(10) Corbin, P. S.; Zimmerman, S. C.; Thiessen, P. A.; Hawryluk, N. A.; Murray, T. J. Complexation-Induced Unfolding of Heterocyclic Ureas. Simple Foldamers Equilibrate with Multiply Hydrogen-Bonded Sheetlike Structures1. *J. Am. Chem. Soc.* **2001**, *123*, 10475−10488.

(11) Kudo, M.; Hanashima, T.; Muranaka, A.; Sato, H.; Uchiyama, M.; Azumaya, I.; Hirano, T.; Kagechika, H.; Tanatani, A. Identification of Absolute Helical Structures of Aromatic Multilayered Oligo(*m*-phenylurea)s in Solution. *J. Org. Chem.* **2009**, *74*, 8154−8163.

(12) Kudo, M.; Katagiri, K.; Azumaya, I.; Kagechika, H.; Tanatani, A. Synthesis and Helical Properties of Aromatic Multilayered Oligoureas. *Tetrahedron* **2012**, *68*, 4455−4463.

(13) Onouchi, H.; Miyagawa, T.; Furuko, A.; Maeda, K.; Yashima, E. Enantioselective Esterification of Prochiral Phosphonate Pendants of a Polyphenylacetylene Assisted by Macromolecular Helicity: Storage of a Dynamic Macromolecular Helicity Memory. *J. Am. Chem. Soc.* **2005**, *127*, 2960−2965.

(14) Emery, R.; Macleod, N. A.; Snoek, L. C.; Simons, J. P. Conformational Preferences in Model Antiviral Compounds: A Spectroscopic and Computational Study of Phenylurea and 1,3-Diphenylurea. *Phys. Chem. Chem. Phys.* **2004**, *6*, 2816−2820.

(15) Badawi, H. M.; Forner, W. Analysis of the Infrared and Raman Spectra of the Symmetrically Substituted 1,3-diphenylurea and 1,3-diphenylacetone. *Spectrochim. Acta, Part A* **2012**, *95*, 435−441.

(16) Hirano, T.; Osaki, T.; Fujii, S.; Komatsu, D.; Asumaya, I.; Tanatani, A.; Kagechika, H. Fluorescent Visualization of the Conformational Change of Aromatic Amide or Urea Induced by N-methylation. *Tetrahedron Lett.* **2009**, *50*, 488−491.

(17) Yamaguchi, K.; Matsumara, G. Aromatic Architecture. Use of the *N*-Methylamide Structure as a Molecular Splint. *J. Am. Chem. Soc.* **1991**, *113*, 5475−5476.

(18) Clayden, J.; Hennecke, U.; Vincent, M. A.; Hillier, I. H.; Helliwell, M. The Origin of the Conformational Preference of *N*,*N*′-Diaryl-*N*,*N*′-dimethylureas. *Phys. Chem. Chem. Phys.* **2010**, *12*, 15056−15064.

(19) Lepore, U.; Castronuovo Lepore, G.; Ganis, P.; Germain, G.; Goodman, M. Conformation of Substituted Arylureas. Crystal Structures of *N*,*N*′-Dimethyl-*N*,*N*′-di(*p*-nitrophenyl)urea and *N*,*N*′-Dimethyl-*N*,*N*′-di(2,4-dinitrophenyl)urea. *J. Org. Chem.* **1976**, *41*, 2134−2137.

(20) Galan, J. F.; Brown, J.; Wildin, J.; Liu, Z.; Liu, D.; Moyna, G.; Pophristic, V. Intramolecular Hydrogen Bonding in *ortho*-Substituted Arylamide Oligomers: A Computational and Experimental Study of *ortho*-Fluoro- and *ortho*-Chloro-*N*-methylbenzamides. *J. Phys. Chem. B* **2009**, *113*, 12809−12815.

(21) Pophristic, V.; Vemparala, S.; Ivanov, I.; Liu, Z.; Klein, M. L.; DeGrado, W. F. Controlling the Shape and Flexibility of Arylamides: A Combined ab Initio, ab Initio Molecular Dynamics, and Classical Molecular Dynamics Study. *J. Phys. Chem. B* **2006**, *110*, 3517−3526.

(22) Becke, A. D. Density-Functional Thermochemistry. III. The Role of Exact Exchange. *J. Chem. Phys.* **1993**, 5648−5652.
(23) Stephens, P. J.; Devlin, F. J.; Chabalowski, C. F.; Frisch, M. J. Ab Initio Calculation of Vibrational Absorption and Circular Dichroism Spectra Using Density Functional Force Fields. *J. Phys. Chem.* **1994**, *98*, 11623−11627.
(24) Frisch, M. J.; Head-Gordon, M.; Pople, J. A. Direct MP2 Gradient Method. *Chem. Phys. Lett.* **1990**, *166*, 275−280.
(25) Head-Gordon, M.; Pople, J. A.; Frisch, M. J. MP2 Energy Evaluation by Direct Methods. *Chem. Phys. Lett.* **1988**, *153*, 503−506.
(26) Saebo, S.; Almlof, J. Avoiding the Integral Storage Bottleneck in LCAO Calculations of Electron Correlation. *Chem. Phys. Lett.* **1989**, *154*, 83−89.
(27) Simon, S.; Duran, M.; Dannenberg, J. J. How does Basis Set Superposition Error Change the Potential Surfaces for Hydrogen Bonded Dimers? *J. Phys. Chem.* **1996**, *105*, 11024−11031.
(28) Boys, S. F.; Bernardi, F. Calculation of Small Molecular Interactions by Differences of Separate Total Energies- Some Procedures with Reduced Errors. *Mol. Phys.* **1970**, *19*, 553.
(29) Andersson, M. P.; Uvdal, P. New Scale Factors for Harmonic Vibrational Frequencies Using the B3LYP Density Functional Method with the Triple-ζ Basis Set 6-311+G(d,p). *J. Phys. Chem. A* **2005**, *109*, 2937−2941.
(30) Frisch, M. J.; Trucks, G. W.; Schlegel, H. B.; Scuseria, G. E.; Robb, M. A.; Cheeseman, J. R.; Scalmani, G.; Barone, V.; Mennucci, B.; Petersson, G. A.; Nakatsuji, H.; Caricato, M.; Li, X.; Hratchian, H. P.; Izmaylov, A. F.; Bloino, J.; Zheng, G.; Sonnenberg, J. L.; Hada, M.; Ehara, M.; Toyota, K.; Fukuda, R.; Hasegawa, J.; Ishida, M.; Nakajima, T.; Honda, Y.; Kitao, O.; Nakai, H.; Vreven, T.; Montgomery, J. A., Jr.; Peralta, J. E.; Ogliaro, F.; Bearpark, M.; Heyd, J. J.; Brothers, E.; Kudin, K. N.; Staroverov, V. N.; Kobayashi, R.; Normand, J.; Raghavachari, K.; Rendell, A.; Burant, J. C.; Iyengar, S. S.; Tomasi, J.; Cossi, M.; Rega, N.; Millam, J. M.; Klene, M.; Knox, J. E.; Cross, J. B.; Bakken, V.; Adamo, C.; Jaramillo, J.; Gomperts, R.; Stratmann, R. E.; Yazyev, O.; Austin, A. J.; Cammi, R.; Pomelli, C.; Ochterski, J. W.; Martin, R. L.; Morokuma, K.; Zakrzewski, V. G.; Voth, G. A.; Salvador, P.; Dannenberg, J. J.; Dapprich, S.; Daniels, A. D.; Farkas, Ö.; Foresman, J. B.; Ortiz, J. V.; Cioslowski, J.; Fox, D. J. *Gaussian 09*, Revision A.1; Gaussian: Wallingford, CT, USA, 2009.
(31) Glendening, E. D.; Landis, C. R.; Weinhold, F. NBO 6.0: Natural Bond Orbital Analysis Program. *J. Comput. Chem.* **2013**, *34*, 1429−1437.
(32) Glendening, E. D.; Badenhoop, J. K.; Reed, A. E.; Carpenter, J. E.; Bohmann, J. A.; Morales, C. M.; Landis, C. R.; Weinhold, F. *NBO 6.0 program*; Theoretical Chemistry Institute, University of Wisconsin: Madison, WI, USA, 2013.
(33) Atkins, P.; de Paula, J. *Physical Chemistry*, 9th ed.; Oxford University Press: Oxford, U.K., 2010.
(34) Wang, J.; Wolf, R. M.; Caldwell, J. W.; Kollman, P. A.; Case, D. A. Development and Testing of a General Amber Force Field. *J. Comput. Chem.* **2004**, *25*, 1157−1174.
(35) Fox, T.; Kollman, P. A. Application of the RESP Methodology in the Parameterization of Organic Solvents. *J. Phys. Chem. B* **1998**, *102*, 8070−8079.
(36) Liu, Z.; Teslja, A.; Pophristic, V. An *ab Initio* Molecular Orbital Study of Intramolecular Hydrogen Bonding in *ortho*-Substituted Arylamides: Implications for the Parameterization of Molecular Mechanics Force Fields. *J. Comput. Chem.* **2011**, *32*, 1846−1858.
(37) Liu, Z.; Remsing, R. C.; Liu, D.; Moyna, G.; Pophristic, V. Hydrogen Bonding in *ortho*-Substituted Arylamides: The Influence of Protic Solvents. *J. Phys. Chem. B* **2009**, *113*, 7041−7044.
(38) Cieplak, P.; Cornell, W. D.; Bayly, C.; Kollman, P. A. Application of the Multimolecule and Multiconformational RESP Methodology to Biopolymers: Charge Derivation for DNA, RNA, and proteins. *J. Comput. Chem.* **1995**, *16*, 1357−1377.
(39) Phillips, J. C.; Braun, R.; Wang, W.; Gumbart, J.; Tajkhoshid, E.; Villa, E.; Chipot, C.; Skeel, R. D.; Kale, L.; Shulten, K. Scalable Molecular Dynamics with NAMD. *J. Comput. Chem.* **2005**, *26*, 1781−1802.
(40) Harris, D. C. *Quantitative Chemical Analysis*, 8th ed.; W. H. Freeman: New York, 2010.
(41) Šponer, J.; Jurečka, P.; Marchan, I.; Luque, F. J.; Orozco, M.; Hobza, P. Nature of Base Stacking: Reference Quantum-Chemical Stacking Energies in Ten Unique B-DNA Base-Pair Steps. *Chem.—Eur. J.* **2006**, *12*, 2854−2865.
(42) Hobza, P.; Šponer, J. Toward True DNA Base-Stacking Energies: MP2, CCSD(T), and Complete Basis Set Calculations. *J. Am. Chem. Soc.* **2002**, *124*, 11802−11808.
(43) Han, Y.-K.; Kim, H.; Son, S.-K.; Lee, Y. S. Effects of Intramolecular Basis Set Superposition Error on Conformational Energy Difference of 1,2-Difluoroethane and 1,2-Dimethoxyethane. *Bull. Korean Chem. Soc.* **2002**, *23*, 1267−1271.
(44) Balabin, R. M. Enthalpy Difference between Conformations of Normal Alkanes: Intramolecular Basis Set Superposiion Error (BSSE) in the Case of *n*-Butane and *n*-Hexane. *J. Chem. Phys.* **2008**, *129*, 164101-1−164101-5.
(45) Kim, K. H.; Kim, J. C.; Han, Y.-K. Effect of Basis set Superposition Error on the MP2 Relative Energies of Gold Cluster Au_6. *Bull. Korean Chem. Soc.* **2009**, *30*, 794−796.
(46) Masson, E. Torsional Barriers of Substituted Biphenyls Calculate using Density Functional Theory: A Benchmarking Study. *Org. Biomol. Chem.* **2013**, *11*, 2859−2871.
(47) Antony, J.; Grimme, S. Density Functional Theory Including Dispersion Corrections for Intermolecular Interactions in a Large Benchmark Set of Biologically Relevant Molecules. *Phys. Chem. Chem. Phys.* **2006**, *8*, 5287−5293.
(48) Burns, L. A.; Vázquez-Mayagoitia, Á.; Sumpter, B. G.; Sherrill, C. D. Density-Functional Approaches to Noncovalent Interactions: A Comparison of Dispersion Corrections (DFT-D), Exchange-Hole Dipole Moment (XDM) Theory, and Specialized Functionals *J. Chem. Phys.* **2011**, *134*, -.
(49) Grimme, S. Semiempirical GGA-type Density Functional Constructed with a Long-Range Dispersion Correction. *J. Comput. Chem.* **2006**, *27*, 1787−1799.
(50) Rajnikant, D.; Deshmukh, M. B. Kamni Synthesis, X-ray structure and N-H···O Interactions in 1,3-Diphenyl-urea. *Bull. Mater. Sci.* **2006**, *29*, 239−242.
(51) Huth, S. L.; Threlfall, T. L.; Hursthouse, M. B. *Crystal Structure Report Archive*; University of Southampton: Southampton, U.K., 2008.
(52) Sudha, L. V.; Sathyanarayana, D. N. Infrared and ^{1}H-NMR Study of Molecular Conformation of Some *N,N′*-Arylalkylureas. *J. Mol. Struct.* **1984**, *125*, 89−96.
(53) Alecu, I. M.; Zheng, J.; Zhao, Y.; Truhlar, D. G. Computational Thermochemistry: Scale Factor Databases and Scale Factors of Vibrational Frequencies Obtained from Electronic Model Chemistries. *J. Chem. Theory Comput.* **2010**, *6*, 2872−2887.
(54) Meier, R. J. On the Art and Science in Curve-Fitting Vibrational Spectra. *Vib. Spectrosc.* **2005**, *39*, 266−269.
(55) Myshakina, N. S.; Ahmed, Z.; Asher, S. A. Dependence of Amide Vibrations on Hydrogen Bonding. *J. Phys. Chem. B* **2008**, *112*, 11873−11877.
(56) Longhi, G.; Abbate, S.; Lebon, F.; Castellucci, N.; Sabatino, P.; Tomasini, C. Conformational Studies of Phe-Rich Foldamers by VCD Spectroscopy and ab Initio Calculations. *J. Org. Chem.* **2012**, *77*, 6033−6042.
(57) Sudha, L. V.; Sathyanarayana, D. N. Conformation of some *N,N′*-arylalkyl thioureas by ^{1}H-NMR and Infrared spectral analysis. *Spectrochim. Acta* **1984**, *40A*, 751−755.
(58) Lepore, G.; Migdal, S.; Blagdon, D. E.; Goodman, M. Conformations of substituted arylureas in solution. *J. Org. Chem.* **1973**, *38*, 2590−2594.